Acta Crystallographica Section F
Structural Biology and Crystallization Communications
ISSN 1744-3091

Use of differential scanning fluorimetry to optimize the purification and crystallization of PLP-dependent enzymes

Todd W. Geders, Kathryn Gustafson and Barry C. Finzel*

Department of Medicinal Chemistry, University of Minnesota, Minneapolis, MN 55455, USA

Correspondence e-mail: finze007@umn.edu

Received 6 March 2012
Accepted 24 March 2012

Differential scanning fluorimetry (DSF) is a practical and accessible technique that allows the assessment of multiphasic unfolding behavior resulting from subsaturating binding of ligands. Multiphasic unfolding is indicative of a heterogenous protein solution, which frequently interferes with crystallization and complicates functional characterization of proteins of interest. Along with UV–Vis spectroscopy, DSF was used to guide purification and crystallization improvements for the pyridoxal 5′-phosphate (PLP) dependent transaminase BioA from *Mycobacterium tuberculosis*. The incompatibility of the primary amine-containing buffer 2-amino-2-(hydroxymethyl)-1,3-propanediol (Tris) and PLP was identified as a significant contributor to heterogeneity. It is likely that the utility of DSF for ligand-binding assessment is not limited to the cofactor PLP but will be applicable to a variety of ligand-dependent enzymes.

1. Introduction

Differential scanning fluorimetry (DSF or ThermoFluor) provides a highly sensitive and practical way to monitor the thermally induced unfolding of protein samples. The method exploits the properties of certain dyes that sharply increase in fluorescence when bound to denatured or partially folded polypeptides (Pantoliano *et al.*, 2001). As a protein solution is warmed, for instance in readily available real-time polymerase chain reaction (RT-PCR) instruments, the equilibrium between properly folded and unfolded polypeptide is shifted such that the preponderance of the dye is captured by the unfolded protein and a strong increase in fluorescence can be observed. The signature melting temperature (T_m) at which this transition occurs is a consequence of the innate thermostability of the protein under the experimental conditions.

The T_m of a protein can shift markedly under different solution conditions that alter the folding equilibrium. For this reason, DSF has found utility as a tool for identifying optimum solution conditions for protein stabilization (Niesen *et al.*, 2007; Mezzasalma *et al.*, 2007) and crystallization (Ericsson *et al.*, 2006). The binding of small molecules can also alter protein stability to denaturation. A ligand-induced shift in the signature T_m (ΔT_m) measured by DSF under conditions where the presence or absence of a small molecule is the only variable constitutes a biophysical method for the detection of ligand binding in fragment screening (Kranz & Schalk-Hihi, 2011; Grasberger *et al.*, 2005; Lo *et al.*, 2004). Under certain experimental conditions, thermal transition data from DSF can even be used to extract thermodynamic parameters of binding (Layton & Hellinga, 2010; Cimmperman *et al.*, 2008).

A correlation between complex multiphasic denaturation behavior and a low likelihood of success in protein crystallization has recently been demonstrated (Dupeux *et al.*, 2011). It has long been recognized that subsaturation binding of ligands to proteins can produce multiphasic unfolding behavior (Shrake & Ross, 1992), but we are unaware of any discussion of how DSF might be used to characterize samples during the preparation and optimization of protein–ligand cocrystals. The optimization of crystallization underlying our recent report of structures of *Mycobacterium tuberculosis* BioA (Shi *et al.*, 2011) illustrates how DSF might be used. BioA, a potential therapeutic target in the causative agent of tuberculosis, is involved in biotin biosynthesis and catalyzes the PLP-dependent transamination of

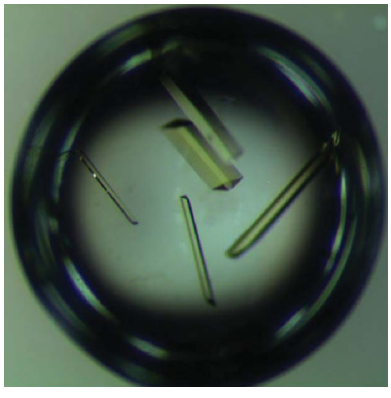

7-keto-8-aminopelargonic acid to 7,8-diaminopelargonic acid using *S*-adenosylmethionine (SAM) as the amino donor (Mann & Ploux, 2006). The observation of multiphasic denaturation of BioA samples led us immediately to recognize a problem with subsaturation of the

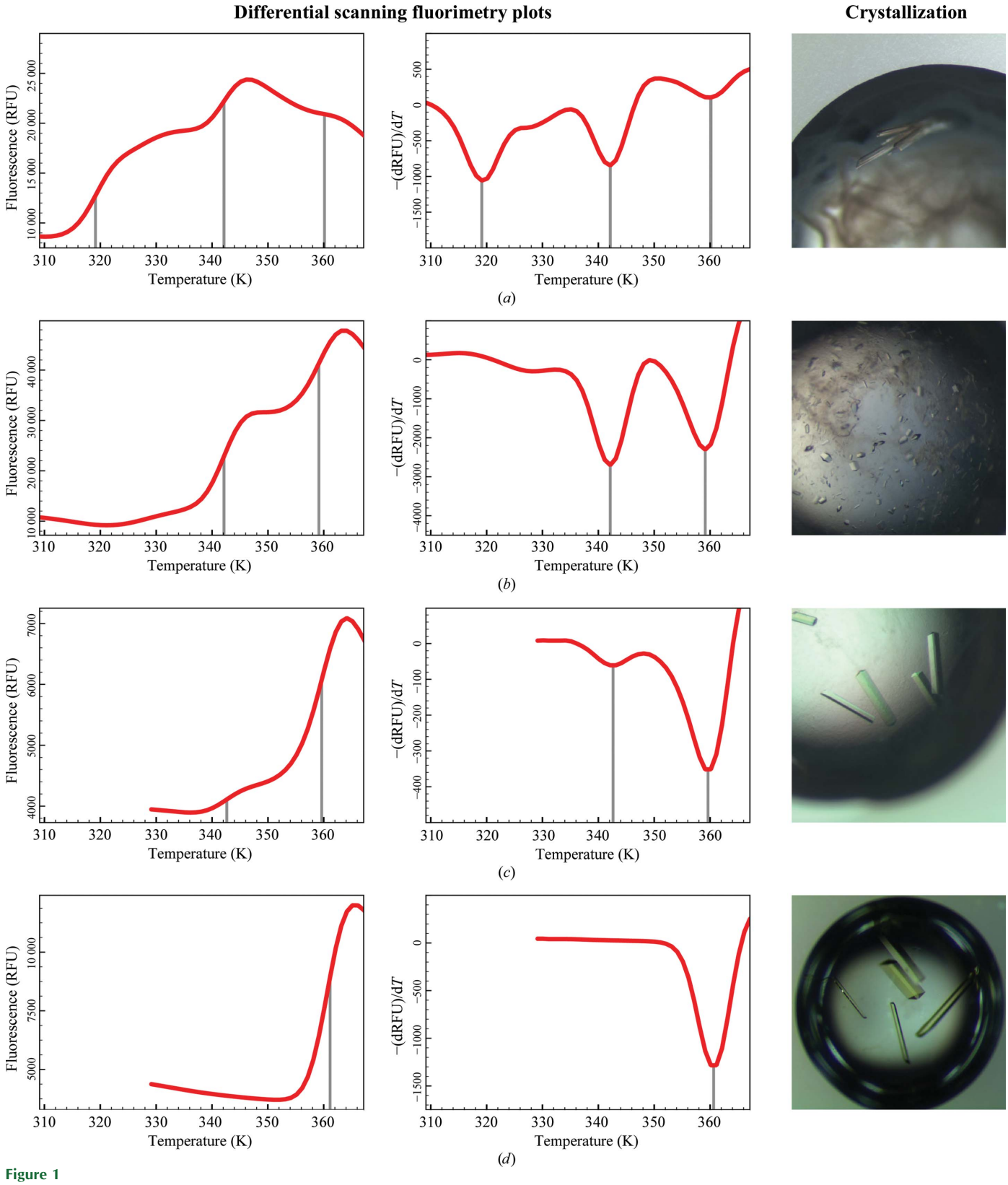

Figure 1
DSF melting curves, their first derivatives and representative crystallization images for the various stages of purification optimization. Transitions at 318, 341 and 359 K correspond to misfolded, apo and PLP-loaded BioA, respectively. (*a*) BioA as purified according to Dey *et al.* (2010) with PLP and Tris in the lysis buffer and Tris and DTT in the storage buffer. (*b*) BioA purified with PLP and HEPES in the lysis buffer and Tris and DTT in the storage buffer. (*c*) BioA purified with PLP and HEPES in the lysis buffer and HEPES and TCEP in the storage buffer. (*d*) BioA purified as in (*c*) but with PLP supplementation prior to final concentration (Shi *et al.*, 2011).

pyridoxal 5′-phosphate (PLP) cofactor in our crystallization milieu. Using a combination of DSF and the well characterized spectroscopy of PLP-dependent enzymes, we were able to identify and eliminate the source of competition for PLP binding and to re-establish conditions under which a fully PLP-saturated homogeneous protein sample could crystallize readily. Although spectroscopy was important to achieving success in this particular study, the DSF alone was diagnostic of the initial heterogeneity and we believe that it may be similarly useful in identifying problems with heterogeneity in a large number of protein–cofactor and protein–ligand crystallization experiments.

2. Materials and methods

2.1. Protein production and purification

M. tuberculosis BioA was initially purified as described previously (Wilson *et al.*, 2011). In brief, a plasmid (pCDD126) encoding N-terminally His-tagged BioA under the control of the *lac* promoter was transformed into *Escherichia coli* Rosetta 2 (DE3) cells (EMD Chemicals) and plated for 72 h at 310 K on Luria–Bertani (LB) agar plates containing 100 µg ml^{-1} ampicillin and 50 µg ml^{-1} chloramphenicol. Cultures in 2 l baffle flasks containing 400 ml Terrific Broth (TB) containing 100 µg ml^{-1} ampicillin and 50 µg ml^{-1} chloramphenicol were grown for 16 h at 310 K and cells were harvested by centrifugation (15 min at 8000*g* at 277 K). Cells from 1 l culture were resuspended in 200 ml 50 m*M* Tris pH 7.6 or (later) HEPES pH 7.5, 500 m*M* NaCl, 1 m*M* $MgCl_2$, 1 mg ml^{-1} lysozyme, 100–400 µ*M* PLP and either 1 m*M* dithiothreitol (DTT) or 0.1 m*M* Tris(2-carboxyethyl)phosphine (TCEP). Cells were sonicated using three cycles of 30 s on and 30 s off at 277 K. Three units of Benzonase (Merck) were added and the lysate was centrifuged for 45 min at 50 000*g*. The supernatant was filtered and loaded onto a 2 × 5 ml HisTrap HP Ni–NTA column (GE Healthcare). The column was washed to baseline with 50 m*M* Tris pH 7.6 or HEPES pH 7.5, 500 m*M* NaCl, 40 m*M* imidazole and eluted with a linear gradient to the same buffer containing 500 m*M* imidazole. Fractions were pooled, concentrated and loaded onto a HiPrep 26/60 Sephacryl S200 HR column (GE Healthcare) equilibrated with either 25 m*M* Tris pH 7.6 or HEPES pH 7.5, 50 m*M* NaCl, 1 m*M* EDTA and either 1 m*M* DTT or 0.1 m*M* TCEP. BioA-containing fractions had either 0 or 1 m*M* PLP added. If 1 m*M* PLP was added, free PLP was removed by 3–5 rounds of concentration and dilution in PLP-free size-exclusion buffer. BioA was concentrated to 10 mg ml^{-1} and stored in 50 µl aliquots at 193 K.

2.2. Differential scanning fluorimetry

Differential scanning fluorimetry was performed using a Bio-Rad CFX96 according to established protocols (Niesen *et al.*, 2007). In brief, purified BioA was diluted at 277 K to give a 40 µl solution consisting of 0.02–0.1 mg ml^{-1} BioA, 25 m*M* HEPES pH 7.5, 50 m*M* NaCl and 5× SYPRO Orange (Life Technologies). To generate the DSF (melting) curve, fluorescence was measured using the FRET channel of the CFX96 between 298 and 368 K with 30 s incubation per 1 K temperature increase. The melting temperature was determined from the peak(s) of the first derivatives of the melting curve; calculations were made using the Bio-Rad *CFX Manager* software and plots were produced using the program *Plot* (http://plot.micw.eu/).

2.3. UV–Vis spectroscopy

A NanoDrop 1000 UV–Vis spectrophotometer (Thermo Scientific) was used for all UV–Vis spectroscopy.

2.4. Crystallization and data collection

All crystallization was performed using the hanging-drop vapor-diffusion method with microseeding at 293 K. Crystals appeared within 24–48 h after mixing 2.0 µl 10 mg ml^{-1} protein solution with 2.0 µl seed-containing reservoir solution and incubating over 1000 µl reservoir solution. Crystal growth was originally attempted using the method (condition *A*) described by Dey *et al.* (2010). When this proved to be unsuccessful with the as-yet unidentified heterogeneous BioA preparation, an alternate condition (condition *B*) was identified *via* high-throughput screening using 20% PEG 6000, 100 m*M* imidazole pH 7.0 as the reservoir solution. Following improvements in BioA homogeneity (see below), a final optimized crystallization condition (condition *C*) was identified that more closely resembled condition *A* but without the Tris buffer. As detailed elsewhere (Shi *et al.*, 2011), condition *C* used a reservoir solution consisting of 8–12% PEG 8000, 100 m*M* $MgCl_2$, 100 m*M* HEPES pH 7.5. In all cases, crystals were soaked in reservoir solution containing 15% PEG 400 and immediately cooled in liquid nitrogen prior to data collection.

To quantify crystal quality and ligand occupancy, diffraction data sets were collected at 100 K using Cu *Kα* radiation on a Rigaku HighFlux HomeLab rotating-anode system in the Kahlert Structural Biology Laboratory at the University of Minnesota. Data were integrated and scaled with *d*TREK* (Pflugrath, 1999). Electron-density maps were calculated from molecular-replacement solutions using the program *Phaser* (McCoy *et al.*, 2007) within *CCP*4 (Winn *et al.*, 2011) with PDB entry 3bv0 (Dey *et al.*, 2010) as a search model. Initial refinement and model building was performed using *REFMAC*5 and *Coot*, respectively (Murshudov *et al.*, 2011; Emsley *et al.*, 2010).

3. Results and discussion

Initial purifications of BioA were performed following the protocol of Dey *et al.* (2010) using the primary amine-containing buffer 2-amino-2-(hydroxymethyl)-1,3-propanediol (Tris) and the thiol-containing reducing agent DTT and with no final supplementation of PLP prior to concentration and storage. Yields were low (<2 mg per litre of culture) and we were unable to reproduce crystals using this material and the published crystallization conditions (Dey *et al.*, 2010). The protein solution was colorless, suggesting very low incorporation of the yellow PLP cofactor. High-throughput crystallization screening yielded a single crystal cluster growing from heavy precipitation (Fig. 1*a*) using a condition consisting of 20% PEG 6000, 100 m*M* imidazole pH 7.0.

The DSF spectrum of this protein possesses multiple melting transitions, with major transitions at 318, 341 and 359 K (Fig. 1*a*). Multiphasic thermal transitions might be anticipated for protein–cofactor systems in which the cofactor is present at subsaturating concentrations. Each species present in the heterogeneous mixture displays a unique characteristic thermal behavior. The transition at 318 K represents relatively unstable species that we tentatively identified as misfolded apo BioA, although this assignment cannot be proven. Whatever it is, crystallization improves as the proportion of protein in this transition is reduced (Fig. 1). In diffraction experiments conducted later, the prevalence of transitions at 341 and 359 K correlated with electron density consistent with apo (no PLP) and holo (covalently bound PLP) BioA, respectively. The low proportion of PLP-bound BioA (T_m = 359 K) and the high proportion of misfolded (T_m = 318 K) and/or apo BioA (T_m = 341 K) is likely to have contributed to the poor crystallization behavior with heavy precipitation. The original crystallization report did note that crystals

Table 1
Data-collection statistics for crystals produced from BioA purified as described in Figs. 1(*a*) (Tris/Tris/DTT), 1(*b*) (HEPES/Tris/DTT) and 1(*c*) (HEPES/HEPES/TCEP).

Data-collection statistics for the crystals in Fig. 1(*d*) have been reported elsewhere (Shi *et al.*, 2011).

Lysis buffer/purification buffer/reducing agent	Tris/Tris/DTT	HEPES/Tris/DTT	HEPES/HEPES/TCEP
Crystallization condition	*B*	*A*	*C*
Space group	$P2_12_12_1$	$P2_12_12_1$	$P2_12_12_1$
Unit-cell parameters (Å)	a = 63.0, b = 66.5, c = 202.8	a = 63.0, b = 66.3, c = 203.0	a = 63.1, b = 66.2, c = 203.1
Resolution (Å)	31.59–2.00 (2.07–2.00)	29.76–2.20 (2.28–2.20)	31.48–2.20 (2.28–2.20)
No. of observed reflections	191544	168934	150134
No. of unique reflections	57457	43930	43696
Completeness (%)	98.2 (91.4)	99.8 (99.1)	99.1 (100)
Average $I/\sigma(I)$	6.5 (2.0)	9.0 (3.2)	18.6 (6.0)
R_{merge}	0.113 (0.328)	0.098 (0.260)	0.146 (0.395)
Average multiplicity	3.33 (2.18)	3.85 (2.52)	3.44 (2.64)

grew from heavy precipitation (Dey *et al.*, 2010). However, in contrast to the original crystallization report, our structural analysis of the crystals that we obtained under condition *B* (see §2.4) revealed a lack of any electron density for PLP within the active site (Table 1 and data not shown).

To improve the crystallization behavior and to ensure PLP loading within BioA, we sought to optimize the purification scheme. In the purification of PLP-dependent enzymes, the PLP concentration is frequently supplemented in the lysis and/or purification buffers to promote full loading of the recombinant protein, including in the reported purification of BioA (Dey *et al.*, 2010). The choice of Tris buffer with PLP supplementation and during enzyme-purification steps was suboptimal, since PLP is known to rapidly react with primary amines (Matsuo, 1957; Buzard & Nytch, 1959; Mitra & Metzler, 1988), including the primary amine of Tris (Fig. 2*a*). The use of Tris with PLP-dependent enzymes is not uncommon. A quick survey of over 600 structure entries in the Protein Data Bank (Berman *et al.*, 2000; http://www.rcsb.org/pdb; accessed 5 December 2011) which include bound PLP revealed that nearly 15% of those which include annotation regarding the crystallization method also identify Tris as the solution buffer. UV–Vis spectroscopy demonstrated that 100 µ*M* PLP added to a buffer containing 100 m*M* Tris had an absorbance maximum near 420 nm, which is characteristic of PLP as a Schiff base and not the free aldehyde (Fig. 2*a*). Solutions containing up to 400 µ*M* PLP in water or HEPES had an absorbance maximum of 390 nm (Fig. 2*a*), indicating that PLP exists as a free aldehyde capable of forming a Schiff base.

By replacing the lysis buffer containing the primary amine-containing Tris with HEPES buffer, which lacks a primary amine, we observed significantly higher PLP loading of BioA, which was reflected in both DSF and UV–Vis spectroscopy (Fig. 1*b*). Whereas the majority of BioA was either misfolded or lacked PLP when purified with Tris/PLP, BioA isolated using HEPES/PLP had roughly equal amounts of apo and holo (PLP-loaded) BioA and none of the low-melting-point species. Additionally, the crystallization behavior was significantly improved; crystals grew more regularly and could be readily obtained using crystallization condition *A* (see §2.4) which was similar to the published PEG 8000 conditions (Dey *et al.*, 2010). The crystals were faintly yellow (Fig. 1*b*). Preliminary structural analysis revealed electron density consistent with PLP, but present at low occupancy (Table 1 and data not shown).

To further improve the homogeneity and crystallization behavior of BioA, Tris was replaced with HEPES in all buffers throughout lysis, nickel-purification and size-exclusion chromatography steps and PLP supplementation was increased to 200 µ*M* during lysis. UV–Vis spectroscopy of material purified using this technique had a peak near 420 nm (Fig. 2*b*) consistent with PLP covalently bound to BioA as a Schiff base. Curiously, a second peak near 345 nm existed for this protein when stored with the common thiol-containing reducing agent dithiothreitol (DTT; Fig. 2*b*). This unidentified peak near 345 nm was also observed for purified BioA when stored in another thiol-containing reducing agent, β-mercaptoethanol (Mann & Ploux, 2006). When the protein was exchanged into a thiol-free solution containing the reducing agent Tris(2-carboxyethyl)phosphine (TCEP), the second peak near 345 nm disappeared. The peak could be

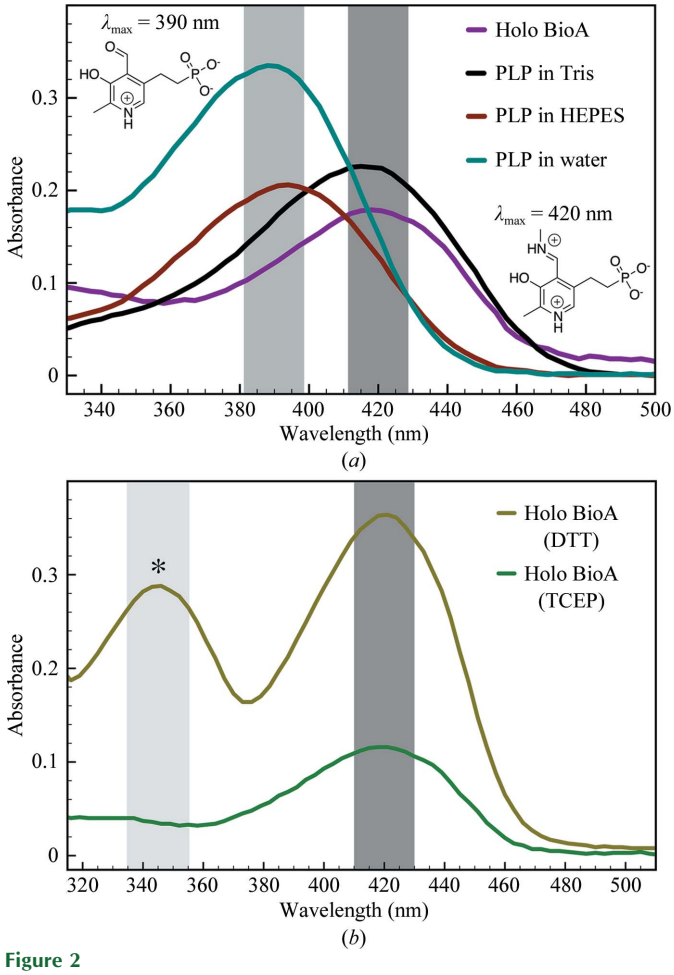

Figure 2
UV–Vis spectroscopy of PLP or PLP-bound (holo) BioA under various conditions. (*a*) Spectra of 200 µ*M* holo BioA (purple), 200 µ*M* PLP in 100 m*M* Tris pH 7.6 (black), 200 µ*M* PLP in 100 m*M* HEPES pH 7.5 (red) and 400 µ*M* PLP in water (cyan). Absorbance maxima at 390 and 420 nm correspond to free-aldehyde or internal-aldimine forms of PLP, respectively. (*b*) Spectra of different concentrations of holo BioA in storage buffer containing 1 m*M* DTT (yellow) or 0.1 m*M* TCEP (green). The peak near 345 nm (marked with an asterisk) is unidentified and occurs when holo BioA is in the presence of a thiol-containing reducing agent.

reformed by the addition of DTT, but was not further identified. To increase the homogeneity and avoid any thiol-related complications, TCEP replaced DTT in all buffers.

When the protein was purified under Tris-free and thiol-free conditions, the DSF spectra of BioA demonstrated a significant enrichment of PLP-loaded BioA, with only minor contamination with apo BioA (Fig. 1*c*). Crystallization behavior was also greatly improved; larger yellow crystals grew in drops containing little precipitation using crystallization condition *C* (Fig. 1*c*). Upon preliminary structural analysis, strong electron density consistent with covalently bound PLP was observed in the active site of these crystals (Table 1 and data not shown).

To eliminate the minor contamination with apo BioA from these preparations, BioA was purified using Tris-free and thiol-free buffers and then incubated with 1 m*M* PLP prior to final concentration. The excess PLP was removed by three cycles of 15-fold dilution/concentration in PLP-free buffers prior to freezing the protein for storage. BioA produced using this technique had a single melting transition at 359 K by DSF and a single UV–Vis peak near 420 nm, indicating homogeneous PLP-loaded BioA (Figs. 1*d* and 2). The final A_{414}/A_{280} ratio for this material was 0.13, which differs from the previously reported value of 0.22 for BioA purified from buffers containing Tris and thiols (Mann & Ploux, 2006). Crystallization produced large intensely yellow crystals that grew in precipitation-free drops.

While the diffraction resolution of individual crystals was not significantly altered during the course of this optimization, the size, the crystal morphology and the regularity with which single crystals suitable for analysis could be produced were greatly improved. The high occupancy of bound PLP constituted an essential improvement required for the *in situ* characterization of a mechanism-based inhibitor of BioA at higher resolution (Shi *et al.*, 2011). The use of DSF to assess cofactor loading and homogeneity of purified BioA allowed the dramatic improvement in crystallization behavior and enabled further studies that were not possible with the initially purified material. The thermodynamic effects of ligand loading efficiency and homogeneity should not be limited to PLP-dependent enzymes. Multiphasic denaturation curves are not always a property of subsaturated protein–ligand complexes, but when present a multiphasic curve should raise concern regarding the likelihood of success in cocrystallization of any complex.

4. Conclusions

Subsaturating concentrations of the PLP cofactor were easily identified in protein samples of BioA used for crystallization by the multiphasic unfolding behavior observed by differential scanning fluorimetry (DSF). Using a combination of DSF monitoring and UV–Vis spectroscopy, Tris buffer has been identified as a contributor to PLP-binding heterogeneity; upon its removal, monophasic thermal unfolding was restored, extensive amorphous protein precipitation of the BioA was eliminated and crystallization was greatly improved. From these observations, we would advocate the routine use of DSF for the characterization of ligand-bound protein samples that resist crystallization. Multiphasic unfolding behavior is a common feature of proteins when ligand-binding sites are not fully saturated (Shrake & Ross, 1992). DSF provides a rapid, convenient and effective means of identifying subsaturating solution conditions that may also correlate with protein heterogeneity and poor crystallization outcomes.

The use of Tris (and other primary amines) should be avoided in the isolation, purification or crystallization of PLP-dependent enzymes. The potential for chemical reaction of the Tris free amine with PLP has been known for many years (Mitra & Metzler, 1988). Nevertheless, Tris is commonly selected for use in routine biochemistry experiments and is a favorite buffer in many commercially available crystallization screens, and has thus crept into common usage. Clearly, the use of Tris has not precluded the possibility of success in the preparation of enzyme cocrystals with PLP; a large number of PLP-dependent enzymes have been successfully cocrystallized with PLP in the presence of Tris. Nevertheless, it seems prudent to use one of a number of different possible buffers in the crystallization of this important class of enzymes.

This work was supported by grants from the NIH NIAID (R01 AI 091790) and the Minnesota Department of Economic and Employment Development. Computational resources provided by the Minnesota Supercomputing Institute are gratefully acknowledged.

References

Berman, H. M., Westbrook, J., Feng, Z., Gilliland, G., Bhat, T. N., Weissig, H., Shindyalov, I. N. & Bourne, P. E. (2000). *Nucleic Acids Res.* **28**, 235–242.
Buzard, J. A. & Nytch, P. D. (1959). *J. Biol. Chem.* **234**, 884–888.
Cimmperman, P., Baranauskienė, L., Jachimovičiūtė, S., Jachno, J., Torresan, J., Michailovienė, V., Matulienė, J., Sereikaitė, J., Bumelis, V. & Matulis, D. (2008). *Biophys. J.* **95**, 3222–3231.
Dey, S., Lane, J. M., Lee, R. E., Rubin, E. J. & Sacchettini, J. C. (2010). *Biochemistry*, **49**, 6746–6760.
Dupeux, F., Röwer, M., Seroul, G., Blot, D. & Márquez, J. A. (2011). *Acta Cryst.* D**67**, 915–919.
Emsley, P., Lohkamp, B., Scott, W. G. & Cowtan, K. (2010). *Acta Cryst.* D**66**, 486–501.
Ericsson, U. B., Hallberg, B. M., DeTitta, G. T., Dekker, N. & Nordlund, P. (2006). *Anal. Biochem.* **357**, 289–298.
Grasberger, B. L. *et al.* (2005). *J. Med. Chem.* **48**, 909–912.
Kranz, J. K. & Schalk-Hihi, C. (2011). *Methods Enzymol.* **493**, 277–298.
Layton, C. J. & Hellinga, H. W. (2010). *Biochemistry*, **49**, 10831–10841.
Lo, M. C., Aulabaugh, A., Jin, G., Cowling, R., Bard, J., Malamas, M. & Ellestad, G. (2004). *Anal. Biochem.* **332**, 153–159.
Mann, S. & Ploux, O. (2006). *FEBS J.* **273**, 4778–4789.
Matsuo, Y. (1957). *J. Am. Chem. Soc.* **79**, 2016–2019.
McCoy, A. J., Grosse-Kunstleve, R. W., Adams, P. D., Winn, M. D., Storoni, L. C. & Read, R. J. (2007). *J. Appl. Cryst.* **40**, 658–674.
Mezzasalma, T. M., Kranz, J. K., Chan, W., Struble, G. T., Schalk-Hihi, C., Deckman, I. C., Springer, B. A. & Todd, M. J. (2007). *J. Biomol. Screen.* **12**, 418–428.
Mitra, J. & Metzler, D. (1988). *Biochim. Biophys. Acta*, **965**, 93–96.
Murshudov, G. N., Skubák, P., Lebedev, A. A., Pannu, N. S., Steiner, R. A., Nicholls, R. A., Winn, M. D., Long, F. & Vagin, A. A. (2011). *Acta Cryst.* D**67**, 355–367.
Niesen, F. H., Berglund, H. & Vedadi, M. (2007). *Nature Protoc.* **2**, 2212–2221.
Pantoliano, M. W., Petrella, E. C., Kwasnoski, J. D., Lobanov, V. S., Myslik, J., Graf, E., Carver, T., Asel, E., Springer, B. A., Lane, P. & Salemme, F. R. (2001). *J. Biomol. Screen.* **6**, 429–440.
Pflugrath, J. W. (1999). *Acta Cryst.* D**55**, 1718–1725.
Shi, C., Geders, T. W., Park, S. W., Wilson, D. J., Boshoff, H. I., Abayomi, O., Barry, C. E., Schnappinger, D., Finzel, B. C. & Aldrich, C. C. (2011). *J. Am. Chem. Soc.* **133**, 18194–18201.
Shrake, A. & Ross, P. D. (1992). *Biopolymers*, **32**, 925–940.
Wilson, D. J., Shi, C., Duckworth, B. P., Muretta, J. M., Manjunatha, U., Sham, Y. Y., Thomas, D. D. & Aldrich, C. C. (2011). *Anal. Biochem.* **416**, 27–38.
Winn, M. D. *et al.* (2011). *Acta Cryst.* D**67**, 235–242.